Stem Cell Reports
Article

ISSCR

OPEN ACCESS

Phosphorylation of Threonine^{343} Is Crucial for OCT4 Interaction with SOX2 in the Maintenance of Mouse Embryonic Stem Cell Pluripotency

Xianmixinuer Abulaiti,[1,6] Han Zhang,[2,3,4,5,6] Aifang Wang,[2,4] Na Li,[2,3,4] Yang Li,[1] Chenchen Wang,[1,2,4,*] Xiaojuan Du,[1] and Lingsong Li[1,2,3,4,5,*]

[1]Department of Cell Biology, School of Basic Medical Sciences, Peking University Health Science Center, Beijing 100191, China
[2]Shanghai Advanced Research Institute, Chinese Academy of Sciences, Shanghai 201210, China
[3]School of Life Science and Technology, ShanghaiTech University, Shanghai 201210, China
[4]University of Chinese Academy of Sciences, Beijing 100049, China
[5]Shanghai Institute of Materia Medica, Chinese Academy of Sciences, Shanghai 201203, China
[6]Co-first author
*Correspondence: wangcc@sari.ac.cn (C.W.), lils@sari.ac.cn (L.L.)
http://dx.doi.org/10.1016/j.stemcr.2017.09.001

SUMMARY

OCT4 is required to maintain the pluripotency of embryonic stem cells (ESCs); yet, overdose-expression of OCT4 induces ESC differentiation toward primitive endoderm. The molecular mechanism underlying this differentiation switch is not fully understood. Here, we found that substitution of threonine^{343} by alanine (T343A), but not aspartic acid (T343D), caused a significant loss of OCT4-phosphorylation signal in ESCs. Loss of such OCT4-phosphorylation compromises its interaction with SOX2 but promotes interaction with SOX17. We therefore propose that threonine^{343}-based OCT4-phosphorylation is crucial for the maintenance of ESC pluripotency. This OCT4-phosphorylation-based mechanism may provide insight into the regulation of lineage specification during early embryonic development.

INTRODUCTION

During early mouse embryonic development, blastocyst formation represents the first lineage specification, segregating trophectoderm from the inner cell mass (ICM). In the blastocyst, ICM cells exposed to the fluid cavity differentiate into primitive endoderm (PE) cells, while the remaining cells adopt epiblast lineage (Boiani and Scholer, 2005; Niwa, 2007; Rossant and Tam, 2009). Embryonic stem cells (ESCs) are derived from ICM cells and are capable of self-renewal (Evans and Kaufman, 1981; Martin, 1981; Thomson et al., 1998). They can differentiate into all cell lineages of the organism and give rise to a live animal if injected into a recipient mouse embryo (Dietrich and Hiiragi, 2007; Smith, 2001). This pluripotency of ESCs is thought to be maintained by pluripotency factors, OCT4, SOX2, and NANOG. Together, these three transcription factors form a regulatory network that guards the pluripotency of ESCs. They activate self-renewal genes and repress molecules essential for initiating lineage differentiation (Boyer et al., 2005). This model is challenged, however, by the observation that a less than 2-fold increase in *Oct4* causes ESCs to differentiate into endoderm and mesoderm (Niwa et al., 2000). In addition, a high-throughput study has identified more pluripotency factors that can also induce ESC differentiation when overexpressed (Ivanova et al., 2006). This evidence suggests a paradox in the current model where increasing the dosage of a pluripotency factor does not guard maintenance of pluripotency.

To resolve this paradox, an alternative hypothesis has been proposed. Instead of acting as guards of pluripotency, these pluripotency factors might induce differentiation of ESCs toward one lineage, while inhibiting differentiation to other lineages (Loh and Lim, 2011; Shu et al., 2013). In this model, whether a pluripotency factor protects pluripotency or initiates differentiation depends on the distinct partners it encounters (Saxe et al., 2009). For example, OCT4 interacts with SOX2 to upregulate *Nanog* in order to protect ESC pluripotency. However, if OCT4 interacts with SOX17, it induces ESCs to differentiate into PE cells. PE differentiation depends on an increase in production of *Pdgf Receptor alpha* (*Pdgfra*) and *Gata6* (Aksoy et al., 2013). Unlike *Pdgfra*, which is directly regulated by SOX17, *Gata6* is not a direct target of OCT4-SOX17. Upregulation of *Gata6* may be due to the downregulation of *Nanog* upon commitment to PE differentiation, since NANOG and GATA6 mutually repress each other (Chazaud and Yamanaka, 2016; Frankenberg et al., 2011). While the dual function of OCT4 is well accepted, it is currently unclear what decides the binding selectivity of OCT4 to SOX2 or SOX17 in the cells.

The most crucial pluripotency factor, OCT4, is a member of the POU domain transcription factor family (Ryan and Rosenfeld, 1997; Sturm et al., 1988). Its hallmark POU domain is critical for DNA binding (Scholer, 1991). The N-terminal domain is rich in proline and acidic amino acid residues, whereas the C-terminal domain is enriched in serine and threonine residues. Regulation of downstream genes by OCT4 has been extensively investigated

(Chen and Daley, 2008), including the effects of OCT4 phosphorylation. Using mass spectrometry, 14 phosphorylation sites have been identified in human OCT4 (Brumbaugh et al., 2012). Functionally, phosphorylation of threonine^{235} and serine^{236} within the homeobox region in human OCT4 (threonine^{228} and serine^{229} in mouse OCT4) negatively regulates its binding to target DNA (Brumbaugh et al., 2012; Swaney et al., 2009). Interestingly, however, another study reported that phosphorylation of OCT4 at the same residue promotes its interaction with the *Nanog* promoter in human embryonic carcinoma cells (Lin et al., 2012; Zhao et al., 2015). In addition, phosphorylation of serine^{12} is essential for OCT4 interaction with the peptidyl prolyl isomerase PIN 1, thereby stabilizing OCT4 and facilitating its transcriptional activity (Nishi et al., 2011). Furthermore, phosphorylation of serine^{111} leads to an increase in ubiquitination and subsequent degradation of OCT4 (Spelat et al., 2012). It was proposed that the C terminus would most likely be phosphorylated (Brehm et al., 1997, 1998, 1999), and such phosphorylation might be important for regulation of OCT4 function (Scholer, 1991; Seet et al., 2006; Vigano and Staudt, 1996). Despite these findings, there have been no reports about phosphorylation of OCT4 at the C terminus, nor any knowledge about the regulation of ESC pluripotency by OCT4 phosphorylation.

In the present study, we identified threonine^{343} to be a phosphorylation residue located at the C terminus of mouse OCT4. Using CRISPR-Cas9-based genome editing, we modified E14 mouse ESCs (wild-type ESCs) to establish T343A ESCs (in which OCT4 has a single amino acid replacement of T343A) as well as T343D ESCs (in which OCT4 has a single amino acid replacement of T343D). With these three lines of ESCs, we investigated whether serine/threonine-based OCT4 phosphorylation would affect pluripotency. We further investigated the molecular mechanisms for how OCT4 phosphorylation regulates the balance between ESC pluripotency and lineage differentiation.

RESULTS

Phosphorylation of Threonine^{343} Is Crucial for the Serine/Threonine-Based Global OCT4-Phosphorylation in Mouse ESCs

Immunoblotting for OCT4 in immunoprecipitate from mouse ESCs using anti-Phos-Ser/Thr antibody has shown that OCT4 is indeed phosphorylated (Figure 1A, middle lane in upper panel). Since the C terminus is rich in serine and threonine residues that may be phosphorylated (Brehm et al., 1997, 1998, 1999; Scholer, 1991; Vigano and Staudt, 1996), we analyzed the candidate phosphorylation residues at the C terminus of mouse OCT4 using NetPhos software (Blom et al., 1999) and compared these residues with that in human OCT4 (Figure 1B, Human). We then replaced each of the seven serine or threonine residues (Figure 1B, Mouse) with alanine to determine the potential site for serine/threonine-based OCT4 phosphorylation. When these mutated OCT4 proteins were introduced in 293T cells, OCT4 or the "modified-OCT4" proteins were immunoprecipitated with anti-OCT4 antibody and then immunoblotted with anti-Phos-Ser/Thr antibody. We found that six of seven modified OCT4 proteins did not show obvious change in the OCT4-phosphorylation signal between wild-type and mutated OCT4 samples (Figures 1C, upper panel, and 1D). To our surprise, the phosphorylation signal was reduced to only 20% of that in the control by a substitution of the residue threonine^{343} with alanine (Figures 1C, upper panel, lane T343A, and 1D, bar T343A). This suggests that phosphorylation of threonine^{343} (phos-OCT4^{T343}) is crucial for serine/threonine-based OCT4 phosphorylation.

To verify phos-OCT4^{T343} is also important in mouse ESCs, we established T343A ESCs (Figure 1E, T343A) and T343D ESCs (Figure 1E, T343D) by genome editing mouse E14 ESCs (Figure 1E, wild-type). We then tested serine/threonine-based OCT4 phosphorylation in these three cell lines. As shown in Figure 1F, the OCT4-phosphorylation signal showed no obvious change in T343D ESCs (Figure 1F, top panel, right lane T343D), while this signal in T343A ESCs (Figure 1F, middle panel, middle lane T343A) showed only 10% of that seen in wild-type ESCs (Figure 1F, bottom panel, left lane wild-type). Since aspartic acid acts as a phosphor mimetic but cannot be phosphorylated in T343D-OCT4, the phosphorylation signal observed in T343D-OCT4 must represent global OCT4-phosphorylation status. Thus, the loss of phosphorylation signaling in T343A-OCT4 suggests that phos-OCT4^{T343} may mediate phosphorylation of OCT4 at other residues in ESCs and is crucial for global serine/threonine-based OCT4 phosphorylation.

Phosphorylation of Threonine^{343} Is Crucial for OCT4 in Protecting ESC Pluripotency

To ask what effect phos-OCT4^{T343} has on the pluripotency of ESCs, we maintained three lines of ESCs in media supplemented with leukemia-inhibitory factor (LIF), which supports ESC self-renewal. After cultivation for 72 hr, the difference in the morphology of ESCs emerged: T343A ESCs displayed differentiated morphology with few compacted colonies (Figure 2A, middle two lanes in both upper and lower panels, arrows). On the other hand, T343D ESCs (Figure 2A, two lanes on the right in both upper and lower panels, T343D) exhibited no difference compared with wild-type ESCs (Figure 2A, two lanes on the left in both

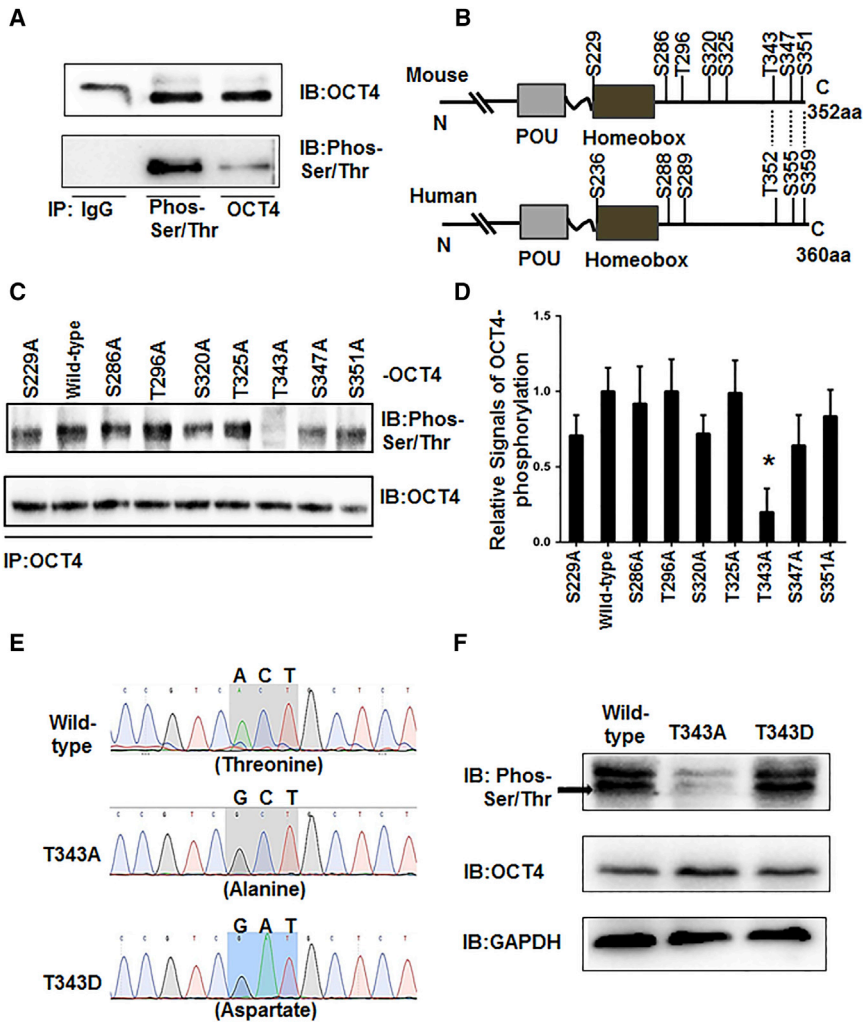

Figure 1. Phosphorylation of Threonine[343] Is Crucial for the Serine/Threonine-Based Global Phosphorylation of OCT4 in Mouse ESCs

(A) Representative immunoblots of anti-OCT4 antibody-immunoprecipitated mouse ESC proteins using anti-Phos-Ser/Thr antibody (lower panel, right lane), and vice versa (upper panel, middle lane). Mouse IgG was used as a control (left two lanes).

(B) Bioinformatics prediction of the potential of serine or threonine residues for phosphorylation in the C terminus of mouse OCT4 protein (upper panel) and mass spectrometry analysis of human OCT4 protein (lower panel). The mouse OCT4 residue serine[229] (upper panel) and serine[236] of human OCT4 (lower panel), located at the homeobox, are also mapped.

(C) Representative immunoblots of anti-OCT4 antibody-precipitated proteins from 293T cells that have been transfected with each of eight mutated *Oct4* molecules (replacing each of eight native residues by alanine as labeled) using anti-OCT4 (lower panel) or anti-Phos-Ser/Thr antibodies (upper panel).

(D) Quantitative measurement of the phosphorylation signal (Figure 1C, upper panels) normalized by each corresponding loaded OCT4 protein (Figure 1C, lower panels). Values represent means ± SD from three independent experiments (*$p < 0.01$; ANOVA).

(E) Sequencing analyses confirmed replacement of the residue threonine[343] by alanine (middle panel) or aspartic acid (lower panel) of OCT4 in mouse ESCs.

(F) Representative immunoblots of OCT4 in wild-type (upper panel, left lane), T343A (upper panel, middle lane) or T343D ESCs (upper panel, right lane) using anti-Phos-Ser/Thr antibody.

upper and lower panels, wild-type). More than 90% of cells in the wild-type (Figure S2, wild-type) or T343D ESCs (Figure S2, T343D) were positive for alkaline phosphatase (ALP) staining, whereas ALP-positive cells in T343A ESCs were reduced to 60% (Figure S2, T343A). This agrees with the flow cytometry analyses that 95% of cells in the wild-type (Figure 2B, left panel, first quadrant) or T343D ESCs (Figure 2B, right panel, first quadrant) were double-positive for OCT4 and SOX2, whereas this number was reduced to 60% in T343A ESCs (Figure 2B, middle panel, first quadrant). The data suggest that about 40% of T343A ESCs ended self-renewal and were undergoing differentiation.

To confirm the effect of OCT4 phosphorylation on ESC pluripotency, we performed quantitative real-time PCR (qRT-PCR) analyses for the expression of pluripotency as well as lineage markers. Compared with wild-type ESCs, *Sox17*, *Gata6*, and *Pdgfra*, markers for PE were significantly increased in T343A ESCs (Figure 2C, Endoderm), whereas the expression of pluripotency genes *Sox2*, *Nanog*, and *Rif1* was significantly reduced (Figure 2C, ESC). In all three ESC lines tested, we saw no significant changes in the expression of *Oct4* (Figure 2C, ESC) or in the expression of mesoderm markers (Figure 2C, Mesoderm) and ectoderm markers (Figure 2C, Ectoderm). Immunofluorescence staining showed that all cells in the wild-type (Figure 2D, left lanes) or T343D ESCs (Figure 2D, right lanes) were positive for OCT4, SOX2, and NANOG but negative for GATA6 (Figure 2D, bottom panel, left and right lanes). In comparison, most T343A ESCs were positive for OCT4 (Figure 2D, top panel, middle lane). About 37% of the cells stained OCT4 positive but SOX2 negative (Figure 2B, middle panel, first quadrant; Figure 2D, top two panels, middle lane, circled).

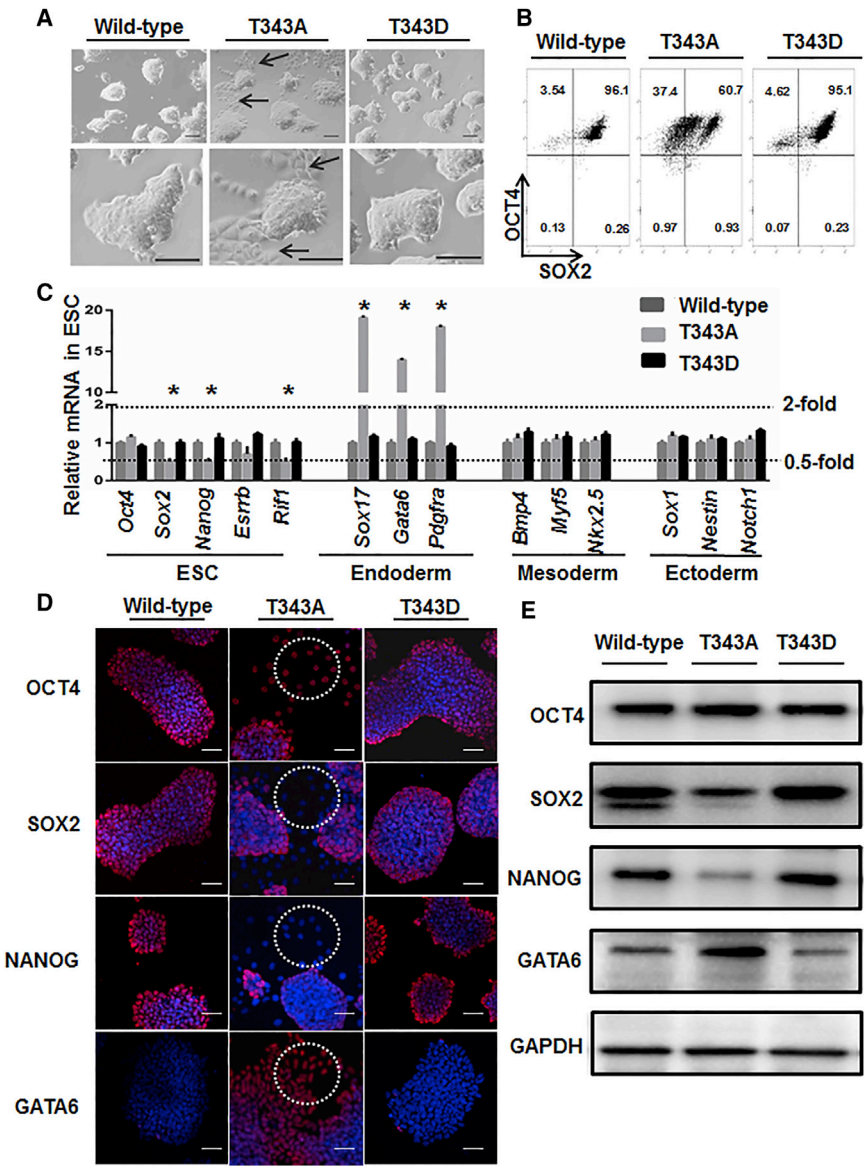

Figure 2. Blockage of OCT4 Phosphorylation at the Residue Threonine^{343} in ESCs Inhibits Self-Renewal and Leads Cells to Differentiation

(A) Representative microscopy of T343A ESCs exhibited cells with few compacted colonies (two lanes in the middle, arrow). In contrast, wild-type (two lanes in the left) and T343D ESCs (two lanes in the right) showed normal compacted colonies (the scale bar represents 100 μm).

(B) Flow cytometry analysis of double-positive cells for OCT4 and SOX2 in T343A, T343D, and wild-type ESCs.

(C) qRT-PCR measurement of mRNA expression for lineage markers in wild-type, T343A, or T343D ESCs, respectively. Values represent means ± SD from three independent biological replicates (*$p < 0.01$; ANOVA).

(D) Immunostaining of T343A, T343D, and wild-type ESCs using antibodies to OCT4, SOX2, NANOG, and GATA6. Cells with differentiated morphology are circled (the scale bar represents 50 μm).

(E) Representative immunoblots of wild-type, T343A, T343D ESCs with the anti-OCT4, anti-SOX2, anti-NANOG and anti-GATA6 antibodies (three independent experiments).

In addition, some T343A ESCs showed GATA6-positive staining (Figure 2D, bottom panel, middle lane, circled) but NANOG-negative staining (Figure 2D, third panel, middle lane, circled). Immunoblotting also confirmed that there was reduced expression of SOX2 and NANOG in T343A ESCs (Figure 2E, middle lanes). In contrast, a crucial endoderm marker of GATA6 expression significantly increased in T343A ESCs (Figure 2E, fourth panel from top, middle lanes) compared with wild-type ESCs (Figure 2E, fourth panel from top, left and right lanes). All these data suggest that loss of OCT4 phosphorylation reduces ESC pluripotency and leads the cells to differentiate toward PE lineage. Therefore, phosphorylation of threonine^{343} is crucial for OCT4 function in the protection of ESC pluripotency.

T343A ESCs Tend to Differentiate to Endoderm and Mesoderm Rather than to Ectoderm

OCT4 is not only required for maintaining ESCs pluripotency but also for regulating lineage specification (Aksoy et al., 2013). To investigate the effect of phos-OCT4^{T343} in lineage commitment, we cultured the three lines of ESCs in embryoid body (EB) differential media. As shown under microscopy, all three ESCs form EBs (Figure 3A). However, H&E staining of the T343A-EB slices, cut in a coronal plane, showed a "diamond ring" shape (Figure 3B, middle lane), suggesting that these cells had differentiated and were undergoing enhanced cavitation to form cystic EBs (Figure 3B, middle lane). This phenomenon was not observed in EBs generated from either wild-type or T343D ESCs (Figure 3B, left and right lanes).

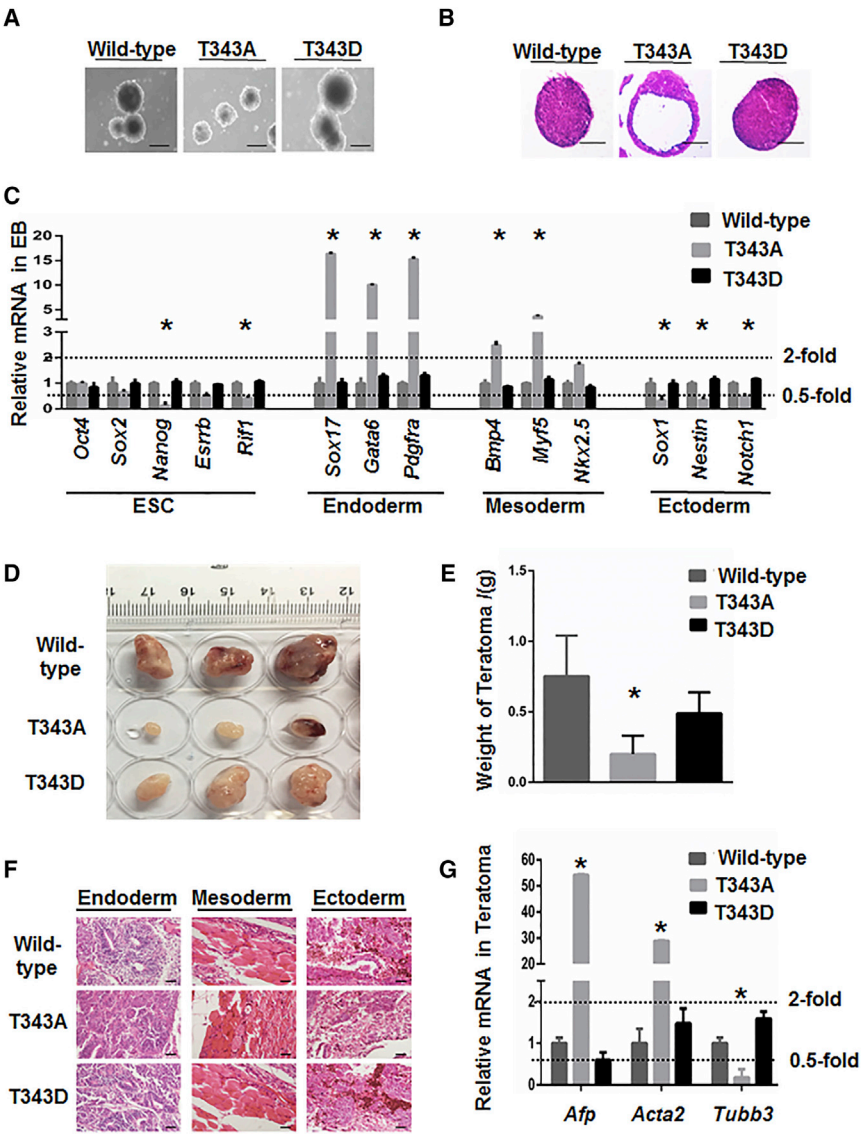

Figure 3. T343A ESCs Tend toward a Skewed Differentiation to Endoderm and Mesoderm Rather than Ectoderm

(A) Analyses of embryoid body formation at day 4 for wild-type (left lane), T343A (middle lane), and T343D (right lane) ESCs (the scale bar represents 100 μm).

(B) H&E staining of sliced embryoid bodies at day 4 for wild-type (left lane), T343A (middle lane), and T343D (right lane) ESCs (the scale bar represents 50 μm).

(C) qRT-PCR analyses of the expression markers for ESCs, endoderm, mesoderm, and ectoderm in embryoid bodies generated from wild-type, T343A, and T343D ESCs. Values represent means ± SD from three independent biological replicates (*$p < 0.01$; ANOVA).

(D) Size of teratoma generated from wide-type (top panel), T343A (middle panel), and T343D (bottom panel) ESCs (n = 3 animals for each condition).

(E) Weight of teratoma generated from wide-type (left bar), T343A (middle bar), and T343D (right bar) ESCs. Values represent means ± SD (n = 3 animals for each condition; *$p < 0.01$; Student's t test).

(F) H&E stains of teratomas generated from wild-type (top panel), T343A (middle panel), and T343D (bottom panel) ESCs indicated sporadic differentiation of ESCs to all three germ layers, including gut-like epithelium (endoderm, left lanes), muscle (mesoderm, middle lanes), and melanin epithelial cells (ectoderm, right lanes) (the scale bar represents 50 μm).

(G) qRT-PCR analyses of the expression markers for endoderm, mesoderm, and ectoderm in teratoma generated from wild-type, T343A, and T343D ESCs. Values represent means ± SD from three independent biological replicates (*$p < 0.01$; ANOVA).

To investigate germ-layer differentiation in EBs, we performed qRT-PCR to measure the expression of pluripotency factors as well as markers for the three germ layers. Compared with EBs derived from either wild-type or T343D ESCs, the T343A ESC-derived EBs showed a significant increase in all the markers for PE, including endoderm markers *Gata6*, *Sox17*, *Pdgfra* as well as mesoderm markers *Bmp4*, *Myf5*, and *Nkx2.5*. In contrast, ectoderm markers such as *Sox1*, *Nestin*, and *Notch1* were significantly reduced in T343A-EBs (Figure 3C). We also investigated the effect of phos-OCT4^{T343} on germ-layer differentiation by a teratoma formation assay. Teratomas derived from T343A ESCs were significantly smaller (Figure 3D) and were only 1/4 the weight (Figure 3E) compared with those generated from the wild-type ESCs. Teratomas from T343D ESCs also showed slightly reduced size (Figure 3D, bottom panel) and weight (Figure 3E, T343D), but the reductions were not statistically significant. In addition, teratomas generated from T343A ESCs contained all three germ layers, including gut-like epithelium (Figure 3F, middle panel, left lane, Endoderm), muscles (Figure 3F, middle panel, middle lane, Mesoderm), and melanin epithelial cells (Figure 3F, middle panel, right lane, Ectoderm). Nonetheless, qRT-PCR analyses indicated that, in teratomas generated from T343A ESCs, the ectoderm markers were decreased (Figures 3G and S3), whereas the markers for endoderm

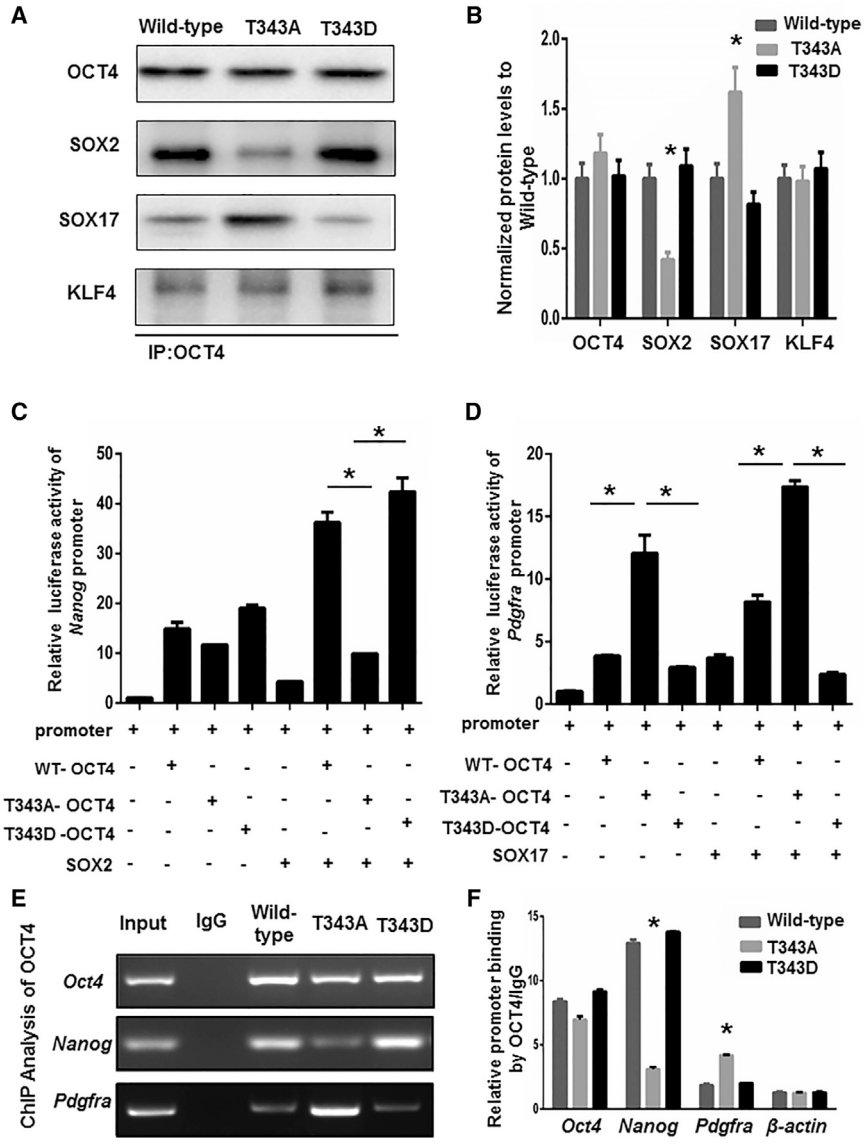

Figure 4. Phosphorylated OCT4 Prefers to Interact with SOX2 while Non-phosphorylated OCT4 Selectively Binds to SOX17

(A) Representative immunoblotting of anti-OCT4 antibody-immunoprecipitated proteins from wild-type, T343A, or T343D ESCs using antibodies to OCT4, SOX2, SOX17, and KLF4.

(B) Quantitative measurement of the immunoblotting signal in T343A (Figure 4A, middle lanes) or T343D (Figure 4A, right lanes) ESCs, normalized by each respective signal in wild-type ESCs (Figure 4A, left lanes). Values represent means ± SD from three independent experiments (*$p < 0.01$; ANOVA).

(C) Luciferase-reporter assay for the *Nanog* promoter. Values represent mean ± SD from three independent replicates (*$p < 0.01$; ANOVA).

(D) Luciferase-reporter assay for the *Pdgfra* promoter. Values represent mean ± SD from three independent replicates (*$p < 0.01$; ANOVA).

(E) ChIP analysis of OCT4 for the promoter of *Oct4*, *Nanog*, and *Pdgfra*.

(F) Relative binding measurement of OCT4 to the promoter of *Oct4*, *Nanog*, and *Pdgfra*. Values represent means ± SD from three independent experiments (*$p < 0.01$; ANOVA).

and mesoderm were increased (Figures 3G and S3, middle bars in left two panels). We therefore conclude that abrogation of the phosphorylation of threonine^{343} leads ESCs to differentiate toward endoderm and mesoderm lineage.

Phos-OCT4^{T343} Prefers to Bind SOX2 while Non-phosphorylated OCT4 Selectively Interacts with SOX17

OCT4 directly interacts with SOX2 to upregulate *Nanog* in the protection of ESC pluripotency. In certain conditions, it partners with SOX17 to induce ESCs to differentiate into PE (Aksoy et al., 2013). To test that OCT4 phosphorylation may serve as a switch for this regulation, we immunoblotted for SOX2, SOX17, and KLF4 in anti-OCT4-immunoprecipitated proteins from each of the three cell lines. As we predicted, phosphorylated OCT4 in wild-type (Figure 4A, left lanes) or T343D ESCs (Figure 4A, right lanes) preferred to bind SOX2 (Figure 4A, second panel from top; Figure 4B, panel SOX2) over SOX17 (Figure 4A, third panel from top; Figure 4B, panel SOX17). In contrast, non-phosphorylated OCT4 (from T343A ESCs) selectively bound SOX17 (Figure 4A, third panel from top, middle lane; Figure 4B, panel SOX17) rather than SOX2 (Figure 4A, second panel from top, middle lane; Figure 4B, panel SOX2). As a control, the binding of KLF4 to all three forms of OCT4 was not affected (Figure 4A, bottom panel; Figure 4B, panel KLF4).

To exclude the possibility that T343A ESCs may contain increased SOX17 but decreased SOX2, we introduced wild-type or the mutant forms of *Oct4* (wild-type *Oct4*, T343A-*Oct4*, and T343D-*Oct4*, respectively) in 293T cells along

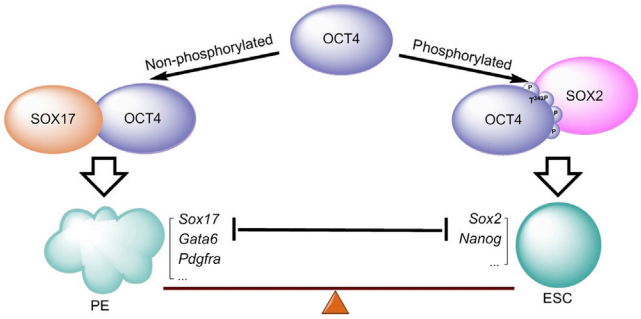

Figure 5. Phos-OCT4^{T343} Serves as a Switch for Regulation of Pluripotency versus Differentiation in ESCs

with both *Sox17*-flag and *Sox2*-flag constructs. As shown in Figure S4, when the input of SOX17 and SOX2 was normalized, T343A-OCT4 bound more SOX17 than T343D or wild-type OCT4 (Figure S4A, top panel; Figure S4B), whereas T343D-OCT4, like wild-type OCT4, preferred to bind to SOX2 (Figure S4A, second panel; Figure S4B). We therefore conclude that, indeed, phos-OCT4^{T343} prefers to bind SOX2, and non-phosphorylated T343A-OCT4 selectively interacts with SOX17.

To measure the effects of selective interaction of OCT4 to its partners on downstream gene expression, we measured the transcriptional activity of *Nanog* and *Pdgfra* promoters, respectively, using a luciferase-reporter approach. We found that, together with SOX2, T343D (Figure 4C, first bar from right) or wild-type OCT4 (Figure 4C, third bar from right), but not with T343A-OCT4 (Figure 4C, second bar from right), significantly activated *Nanog* promoter activity (Figure 4C). In contrast, combination of SOX17 along with T343A-OCT4 (Figure 4D, second bar from right), but not with T343D-OCT4 (Figure 4D, first bar from right), significantly activated *Pdgfra* promoter activity (Figure 4D).

To investigate whether OCT4-SOX2 interaction would enhance the binding of OCT4 to *Nanog* promoter, we therefore performed chromatin immunoprecipitation (ChIP). As shown, OCT4 in wild-type (Figure 4E, third lane from right; Figure 4F) or T343D ESCs (Figure 4E, first lane from right; Figure 4F) prefers to bind to the *Nanog* promoter (Figure 4E, middle panel; Figure 4F, bars *Nanog*) over the *Pdgfra* promoter (Figure 4E, bottom panel; Figure 4F, bars *Pdgfra*), while the OCT4 in T343A ESCs selectively binds to the *Pdgfra* promoter (Figure 4E, bottom panel; Figure 4F, bars *Pdgfra*) rather than the *Nanog* promoter (Figure 4E, middle panel; Figure 4F, bars *Nanog*). These data suggest that phosphorylated OCT4 prefers to bind SOX2 while non-phosphorylated OCT4 selectively binds to SOX17. In addition, the OCT4-SOX2 interaction enhances the binding of OCT4 to the *Nanog* promoter, and OCT4-SOX17 interaction promotes the binding of OCT4 to the *Pdgfra* promoter. We therefore conclude that this OCT4-phosphorylation-based status switch mechanism plays a role in guarding the balance of pluripotency versus differentiation in ESCs (Figure 5A).

DISCUSSION

OCT4 is the most crucial transcription factor required for regulating ESC pluripotency. Whether phosphorylation of OCT4 is involved in this regulation is largely unclear (Hutchins and Robson, 2009; Saxe et al., 2009; Swaney et al., 2009). In the present study, we have identified threonine^{343} to be a phosphorylation residue located at the C terminus of the mouse OCT4 site. In addition, phosphorylation of threonine^{343} is crucial for mediating global OCT4 phosphorylation and is important for the protection of ESC pluripotency. Blockage of phosphorylation at this residue leads to skewed differentiation to PE rather than to ectoderm. Moreover, phos-OCT4^{T343} prefers to interact with SOX2 and upregulates *Nanog* expression, thus maintaining ESC pluripotency. On the contrary, the non-phosphorylated OCT4 binds to SOX17 to promote *Pdgfra* expression, leading to increased expression of *Gata6* in ESCs (Figure 5A). Based on these observations, we predicted that phos-OCT4^{T343} facilitates the lineage commitment of ESCs to ectoderm fate versus PE differentiation.

Functionally, there are four OCT4-phosphorylation sites that have been identified: threonine^{228} and serine^{229} residues in the mouse OCT4 homeobox (Brumbaugh et al., 2012; Swaney et al., 2009); and serine^{12} and serine^{111} residues in the N terminus of human OCT4. In this study, we identified threonine^{343} to be an important phosphorylation residue located at the C terminus of mouse OCT4. We found that abrogation of the phosphorylation of threonine^{343} leads ESCs to differentiate toward PE lineage. This supports previous speculation that the C terminus is most probably phosphorylated (Brehm et al., 1997, 1998, 1999) and may play a role in the regulation of the biological function of OCT4 (Scholer, 1991; Seet et al., 2006; Vigano and Staudt, 1996).

It is noted that substitution of threonine^{343} by alanine, but not aspartic acid, abolishes about 90% of the serine/threonine-based OCT4-phosphorylation signal in mouse ESCs (Figure 1E). Since aspartic acid acts as a phosphor mimetic, T343D cannot be phosphorylated in T343D-OCT4. The phosphorylation signal observed in T343D-OCT4 must represent the global OCT4-phosphorylation status. Thus, the loss of phosphorylation signaling in T343A-OCT4 raises two possibilities: substitution of threonine^{343} by alanine leads to such a significant alteration in the structure of OCT4 protein that most serine/threonine-based phosphorylation no longer happens; or,

phosphorylation of threonine^{343} may mediate phosphorylation of OCT4 at other residues. The fact that T343A-OCT4 binds to SOX17 well in upregulation of *Pdgfra* gene expression in cells (Figures 4A and 4B) suggests that T343A-OCT4 remains as a "normal" structure as non-phosphorylated OCT4^{T343}. The data also imply that T343D-OCT4 may be able to mimic phos-OCT4^{T343} to mediate phosphorylation of OCT4 at other residues.

It has been reported that truncation of the C-terminal domain led to a significant loss of OCT4 phosphorylation (Niwa et al., 2002). To look for other residues with potential for phosphorylation, we further replaced each of all 15 C-terminal serine or threonine residues with alanine (including seven replacements described in Figure 1B) in OCT4 protein (Figure S1A). We introduced these mutated *Oct4* genes in 293T cells, immunoprecipitated the mutated OCT4 protein using anti-OCT4 antibodies, and then immunoblotted the proteins using anti-Phos-Ser/Thr antibody. As reported (Niwa et al., 2002), the mutant OCT4-ΔC (Figure S1A, middle panel) barely showed any phosphorylation signal (Figures S1B and S1C, second lane from left, ΔC). Among the 15 serine/threonine residues, only T343A-OCT4 showed a significant decrease (Figures S1B and S1C, fourth lane from right), whereas the other 14 replacements did not show significant decrease in phosphorylation signal (Figures S1B and S1C). However, when all 14 serine/threonine residues except threonine^{343} were substituted for alanine (Figure S1A, OCT4-$C_{mutation}$), we observed that the phosphorylation signal (mostly phosphorylation of threonine^{343}) in the OCT4-$C_{mutation}$ protein was only 35% of that in the wild-type OCT4 (Figures S1B and S1C, last lane from right, OCT4-$C_{mutation}$). These data suggest that phosphorylation of threonine^{343} may mediate global OCT4 phosphorylation.

With regard to the molecular mechanism of OCT4 in the regulation of ESCs pluripotency, the "guarding model" (Avilion et al., 2003; Chambers et al., 2003; Jaenisch and Young, 2008; Mitsui et al., 2003; Nichols et al., 1998; Scholer et al., 1990; Silva and Smith, 2008; Young, 2011) emphasizes the necessity of OCT4, SOX2, and NANOG pluripotency factors. For instance, a loss of any of these three pluripotency factors leads ESCs to differentiation (Lessard and Crabtree, 2010). An alternative "balance model" describes the sufficiency of these factors in the protection of ESC pluripotency (Loh and Lim, 2011; Shu et al., 2013). Since overexpression of OCT4, for example, induces PE differentiation rather than protects ESC pluripotency, it is the precise level of OCT4 protein that governs the three distinct fates of ESCs (Niwa et al., 2000). An ideal platform to test these two models would, for example, be to modulate OCT4 phosphorylation rather than its protein level, and then examine the effect on ESCs pluripotency. Our T343A and T343D ESCs provide a good system for such investigation, because we could alter OCT4 function with no change in the level of OCT4 protein in ESCs. Using this system, we have found that phos-OCT4^{T343} is indeed crucial for OCT4 in the protection of the pluripotency; an inhibition of such phosphorylation would induce ESC differentiation toward PE. Our data favor the "balanced model" (Figure 5) in which these pluripotency factors are actually lineage specifiers. They regulate differentiation of ESCs toward a specific lineage while inhibiting commitment to other lineages (Figure 3).

In addition to its function in the regulation of ESC pluripotency, OCT4 also plays a role in determining the fate of ICM cells in commitment to either PE or epiblast lineages in the embryo blastocyst. OCT4 works with SOX2 to upregulate *Nanog*, therefore inducing ESC differentiation toward epiblast cells. However, ESCs differentiate into PE if OCT4 interacts with SOX17 (Aksoy et al., 2013). Using T343A and T343D ESCs cultured in differentiation media with no addition of LIF, we discovered that phos-OCT4^{T343} prefers to bind to SOX2 in wild-type as well as in T343D ESCs (Figure 4A, right panel, line 2). On the contrary, non-phosphorylated OCT4 selectively interacts with SOX17 in T343A ESCs (Figure 4A, right panel, line 4). The binding of OCT4 to KLF4 was indifferent to OCT4 phosphorylation (Figure 4A, right panel, line 3). The selective binding of OCT4 to SOX2 over SOX17 was further supported by the skewed differentiation results: T343A ESCs tend to differentiate to endoderm and mesoderm (Figure 3, T343A) compared with T343D and wild-type ESCs (Figure 3, wild-type and T343D). This was demonstrated in both *in vitro* EB differentiation (Figures 3A–3C) and *in vivo* teratoma formation assays (Figures 3D–3F). Based on these observations, we propose that phosphorylation of threonine^{343} determines the binding partner of OCT4, SOX2 or SOX17, thus serving as a lineage switch for ICM cells to epiblast versus PE commitment (Figure 5) during early embryonic development. Furthermore, why phosphorylation of threonine^{343} determines the selectivity of OCT4 to SOX2 over SOX17 merits future investigation.

In our study, phosphorylation of OCT4 at the C terminus was initially studied in human 293T cells transfected with OCT4 or OCT4-like molecules (Figures 1C and 1D). The residue threonine^{343} was selected because of the substitution of this residue by alanine abolishing about 80% of serine/threonine-based OCT4 phosphorylation (Figures 1C and 1D). The replacement of other serine/threonine residues (Figure 1B) at the C terminus did not show significant changes in the phosphorylation signal, but we cannot exclude the possibility that they may be phosphorylated in ESCs. Nonetheless, the conclusion still holds true since T343A ESCs lost 90% of the OCT4-phosphorylation signal (Figure 1F, lane T343A). This suggests that phosphorylation of threonine^{343} is crucial for global OCT4 phosphorylation.

Phosphorylation of theonine^{343} is important for OCT4 in the protection of ESC pluripotency. Why is T343D-OCT4, which cannot be phosphorylated, able to support ESC self-renewal? A possible interpretation is that T343D-OCT4 shares a very similar structure to that of phos-OCT4^{T343}. This is supported by our observation that T343D-OCT4 interacted with SOX2 as efficiently as the wild-type OCT4 (Figures 4A and 4B).

The residue threonine^{343} in mouse OCT4 most likely corresponds to either threonine^{351} or threonine^{352} in human OCT4. The residue threonine^{352} was included in the mass spectrometry phosphorylation study of human OCT4 (Brumbaugh et al., 2012; Swaney et al., 2009). Threonine^{351} has yet to be reported. There are many questions that remain to be resolved. For instance, in addition to serine/threonine-based phosphorylation, does tyrosine-based phosphorylation happen to OCT4 in ESCs? What signaling pathway is involved in the regulation of OCT4 phosphorylation in ESCs? In addition, a large-scale mass spectrometry study of OCT4-phophorylation in mouse ESCs is needed to confirm our discovery.

In summary, we found that phosphorylation of threonine^{343} is crucial for mediating global OCT4 phosphorylation. We provide evidence that phos-OCT4^{T343} interacts with SOX2 to govern ESC pluripotency, whereas non-phosphorylated OCT4^{T343} partners with SOX17 to induce ESC differentiation. Our study also provides insight into the corresponding *in vivo* mechanism by which OCT4 phosphorylation regulates the lineage specification of ICM cells during early embryonic development.

EXPERIMENTAL PROCEDURES

Cell Culture

Mouse E14TG2a cells (ESCs) were maintained on gelatin-coated plates in DMEM (high glucose; HyClone). The medium was supplemented with 20% fetal bovine serum (FBS; BioIndustry), 100 U/mL penicillin/streptomycin (HyClone), 0.1 mM nonessential amino acids (Life Technologies), 0.1 mM β-mercaptoethanol (Sigma), 1 mM sodium pyruvate (Life Technologies), 2 mM L-glutamine (Life Technologies), and 1000 U/mL LIF (Millipore). 293T cells were maintained in DMEM containing 10% FBS.

Point Mutation of *Oct4*

The *Oct4* mutant was amplified by PCR and sub-cloned into pBK vector at EcoRI/XhoI restriction sites. The point mutation was generated using a QuikChange Site-Directed Mutagenesis Kit (Stratagene) according to the manufacturer's instructions. All mutations were verified by DNA sequencing.

Site Mutation of Threonine^{343} of OCT4 in ESC by CRISPR-Cas9

Substitution of threonine^{343} by alanine or aspartic acid was made by CRISPR-Cas9 editing. The 20 bp guide RNA sequence containing the motif *NGG* nearby threonine^{343} (CTC TGT TCC CGT CAC TGC TCT GG) was inserted into PX458 (Addgene plasmid no. 48138) vector at the BbsI site, and then was transfected into ESCs together with Oligo-A^{343} (CAG TCC CTT TTC CTG AGG GCG AGG CCT TTC CCT CTG TTC CCG TCG CTG CTC TGG GCT CTC CCA TGC ATT CAA ACT GAG GCA CCA GCC CT) or Oligo-D^{343} (CAG TCC CTT TTC CTG AGG GCG AGG CCT TTC CCT CTG TTC CCG TCG ATG CTC TGG GCT CTC CCA TGC ATT CAA ACT GAG GCA CCA GCC CT) by jetPEI (Polyplus). GFP positive cells were sorted by flow cytometry (BD FACSAriaIII) 36 hr after transfection. Single cell clones were identified by DNA sequencing. Three cell clones for each genotype were selected for experiments.

Immunoprecipitation and Detection of OCT4 Phosphorylation

ESCs were fixed in 1% paraformaldehyde for 10 min, washed with PBS, and then collected in lysis buffer (50 mM Tris [pH 7.4], 150 mM NaCl, 1% Triton X-100, inhibitors for proteinase and phosphatase). The cell lysates were incubated at 4°C with anti-OCT4 antibody (sc-5279, Santa Cruz Biotechnology) or anti-Phos-Ser/Thr antibody (9381, Abcam), along with protein G Sepharose beads (Millipore) overnight. Each sample was washed four times with lysis buffer and then boiled for 10 min in 40 μL of 2× SDS loading buffer supplemented with 5% β-mercaptoethanol. After centrifugation at 2,000 × *g* for 3 min, supernatants were separated on 10% SDS-PAGE gel and blotted onto NC membrane. Anti-Phos-Ser/Thr (NC9080, Cell Signaling Technology), anti-OCT4 (sc-5279, Santa Cruz), anti-SOX2 (sc-17320, Santa Cruz), SOX17 (24903-1-AP, Proteintech), and anti- KLF4 (ab72543, Abcam) antibodies were used for immunoblotting. Horseradish peroxidase (HRP)-conjugated anti-rabbit (7076S, CST) or anti-mouse (7074S, CST) antibodies were used as the secondary antibody. The images were visualized by the Bio-Ras ChemiDoc XRS+ system.

The site-directed mutated *Oct4* constructs were transfected into 293T cells using jetPEI (Polyplus). Forty-eight hours later, 293T cells were collected. Each mutated OCT4 protein was immunoprecipitated with anti-OCT4 antibodies and then subjected to immunoblotting with anti-Phos-Ser/Thr antibody.

Immunoblot Analysis

Cells were harvested in 150 μL of lysis buffer (50 mM Tris-HCl [pH 7.5], 150 mM NaCl, 0.5% sodium deoxycholate, 1% NP-40) supplemented with complete protease inhibitors (Sigma) and phosphatase inhibitors (Roche). Cell lysates were separated on 10% SDS-PAGE and blotted onto an NC membrane. The membrane was then blocked in 5% nonfat milk and incubated with primary antibodies. Anti-Phos-Ser/Thr (NC9080, CST), anti-OCT4 (sc-5279, Santa Cruz), anti-SOX2 (sc-17320, Santa Cruz), anti-SOX17 (24,903-1-AP, Proteintech), anti-NANOG (ab80892, Abcam), and anti-GATA6 (55,435-1-AP, Proteintech) antibodies were used for immunoblotting. HRP-conjugated anti-mouse (7074S, CST), anti-rabbit (7076S, CST), or anti-goat (7073S, CST) antibodies were used as the secondary antibody. The images were visualized using the Bio-Rad ChemiDoc XRS+ system.

RNA Isolation, RT-PCR, and Real-Time PCR

Total RNA was extracted from cells or teratomas using the MiniBEST Universal RNA Extraction Kit (Takara). RT-PCR was performed using the PrimeScript RT Master Mix (Takara). The expression of genes was detected by qRT-PCR (Applied Biosystems) using SYBR Premix Ex Taq II (Takara). The expression of genes was normalized to that of the internal control *Gapdh*. The data were analyzed by ANOVA with multiple comparisons of the means in GraphPad Prism 5. The results of qRT-PCR are shown as means ± SD from three independent biological replicates. Primers are listed in Table S1.

ChIP qRT-PCR

Chromatin immunoprecipitation (ChIP) was performed as described previously (Soldner et al., 2016). Crosslinks were reversed overnight. RNA and protein were digested using RNase A and Proteinase K, respectively, and DNA was purified with phenol-chloroform extraction and ethanol precipitation. Target-specific binding was analyzed by qRT-PCR (Applied Biosystems) using SYBR Premix Ex Taq II (Takara). Primers are listed in Table S2.

Teratoma Assay

ESCs were harvested, suspended in PBS, and injected subcutaneously into SCID mice (3×10^6 cells per mouse). Four weeks after the injection, tumors were dissected, fixed in 4% paraformaldehyde, embedded in paraffin, and examined by staining with H&E. The paired samples t test was used to analyze the teratoma data. All animal handling and procedures were approved by the Institutional Animal Care and Use Committee at the Peking University Health Science Center.

Luciferase Assays

All cells were seeded in a 24-well plates and transfected with *Nanog* or *Pdgfra* promoter reporter along with *Oct4* or with the mutated *Oct4* gene using jetPEI (Polyplus). Forty-eight hours after transfection, cells were lysed in Passive Lysis Buffer (Promega). Luciferase activity was measured using the Dual Luciferase-Reporter Assay System (Promega).

Embryoid Body Formation

ESCs were cultured in suspension in Petri dishes in ESC growth medium without LIF to form aggregates. At various time points, images were recorded, and the aggregates were harvested for qRT-PCR and histological analysis.

Immunofluorescence Staining

ESCs were grown on glass coverslips (Fisher Scientific) and stained as previously described (Wang et al., 2015).

Statistical Analysis

All quantitative data are presented as means ± SD unless indicated otherwise. The statistical significance of compared measurements was assessed using ANOVA and $p < 0.01$ was considered significant (*).

SUPPLEMENTAL INFORMATION

Supplemental Information includes five figures and two tables and can be found with this article online at http://dx.doi.org/10.1016/j.stemcr.2017.09.001.

AUTHOR CONTRIBUTIONS

The study was conceived and designed by L.L., C.W., and X.A. The ESC lines were generated by H.Z. Bioinformatics analyses and point mutation of OCT4 were carried out by H.Z. and Y.L. All other experiments, including co-immunoprecipitation, immunoblot analysis, teratoma assay, luciferase analysis, and immunofluorescence, were performed by H.Z, X.A., and A.W. Schematic diagrams were designed by N.L. and L.L. The study was supervised by L.L. and C.W. The manuscript was written by L.L, X.A., H.Z., and X.D.

ACKNOWLEDGMENTS

We thank Byron Lee (MIT), Jenny Wu (MIT), and Lingheng Li (Stowers Institue for Medical Research) for their critical comments and Shaorong Gao and Jingsong Li for their technical support. In addition, we thank Yuejin Hua (Zhejiang University), Jianhua Zhu (Fudan University), and Yinan Liu (Peking University) for providing materials. This work was supported by the 863 Program (grant no. 2015AA020303) from the Ministry of Science and Technology of China, a special grant from the Zhang Jiang National Innovation and Shanghai Bureau of Science and Technology (grant no. ZJ2014-ZD-002), and grants from the National Natural Science Foundation of China (grant nos. 31671217, 31000653, 31571517).

Received: March 14, 2017
Revised: August 31, 2017
Accepted: September 1, 2017
Published: October 5, 2017

REFERENCES

Aksoy, I., Jauch, R., Chen, J., Dyla, M., Divakar, U., Bogu, G.K., Teo, R., Leng Ng, C.K., Herath, W., Lili, S., et al. (2013). Oct4 switches partnering from Sox2 to Sox17 to reinterpret the enhancer code and specify endoderm. EMBO J. *32*, 938–953.

Avilion, A.A., Nicolis, S.K., Pevny, L.H., Perez, L., Vivian, N., and Lovell-Badge, R. (2003). Multipotent cell lineages in early mouse development depend on SOX2 function. Genes Dev. *17*, 126–140.

Blom, N., Gammeltoft, S., and Brunak, S. (1999). Sequence and structure-based prediction of eukaryotic protein phosphorylation sites. J. Mol. Biol. *294*, 1351–1362.

Boiani, M., and Scholer, H.R. (2005). Regulatory networks in embryo-derived pluripotent stem cells. Nat. Rev. Mol. Cell Biol. *6*, 872–884.

Boyer, L.A., Lee, T.I., Cole, M.F., Johnstone, S.E., Levine, S.S., Zucker, J.P., Guenther, M.G., Kumar, R.M., Murray, H.L., Jenner, R.G., et al. (2005). Core transcriptional regulatory circuitry in human embryonic stem cells. Cell *122*, 947–956.

Brehm, A., Ohbo, K., and Scholer, H. (1997). The carboxy-terminal transactivation domain of Oct-4 acquires cell specificity through the POU domain. Mol. Cell. Biol. *17*, 154–162.

Brehm, A., Ovitt, C.E., and Scholer, H.R. (1998). Oct-4: more than just a POUerful marker of the mammalian germline? APMIS *106*, 114–124, discussion 124–6.

Brehm, A., Ohbo, K., Zwerschke, W., Botquin, V., Jansen-Durr, P., and Scholer, H.R. (1999). Synergism with germ line transcription factor Oct-4: viral oncoproteins share the ability to mimic a stem cell-specific activity. Mol. Cell. Biol. *19*, 2635–2643.

Brumbaugh, J., Hou, Z., Russell, J.D., Howden, S.E., Yu, P., Ledvina, A.R., Coon, J.J., and Thomson, J.A. (2012). Phosphorylation regulates human OCT4. Proc. Natl. Acad. Sci. USA *109*, 7162–7168.

Chambers, I., Colby, D., Robertson, M., Nichols, J., Lee, S., Tweedie, S., and Smith, A. (2003). Functional expression cloning of Nanog, a pluripotency sustaining factor in embryonic stem cells. Cell *113*, 643–655.

Chazaud, C., and Yamanaka, Y. (2016). Lineage specification in the mouse preimplantation embryo. Development *143*, 1063–1074.

Chen, L., and Daley, G.Q. (2008). Molecular basis of pluripotency. Hum. Mol. Genet. *17*, R23–R27.

Dietrich, J.E., and Hiiragi, T. (2007). Stochastic patterning in the mouse pre-implantation embryo. Development *134*, 4219–4231.

Evans, M.J., and Kaufman, M.H. (1981). Establishment in culture of pluripotential cells from mouse embryos. Nature *292*, 154–156.

Frankenberg, S., Gerbe, F., Bessonnard, S., Belville, C., Pouchin, P., Bardot, O., and Chazaud, C. (2011). Primitive endoderm differentiates via a three-step mechanism involving Nanog and RTK signaling. Dev. Cell *21*, 1005–1013.

Hutchins, A.P., and Robson, P. (2009). Unraveling the human embryonic stem cell phosphoproteome. Cell Stem Cell *5*, 126–128.

Ivanova, N., Dobrin, R., Lu, R., Kotenko, I., Levorse, J., DeCoste, C., Schafer, X., Lun, Y., and Lemischka, I.R. (2006). Dissecting self-renewal in stem cells with RNA interference. Nature *442*, 533–538.

Jaenisch, R., and Young, R. (2008). Stem cells, the molecular circuitry of pluripotency and nuclear reprogramming. Cell *132*, 567–582.

Lessard, J.A., and Crabtree, G.R. (2010). Chromatin regulatory mechanisms in pluripotency. Annu. Rev. Cell Dev. Biol. *26*, 503–532.

Lin, Y., Yang, Y., Li, W., Chen, Q., Li, J., Pan, X., Zhou, L., Liu, C., Chen, C., He, J., et al. (2012). Reciprocal regulation of Akt and Oct4 promotes the self-renewal and survival of embryonal carcinoma cells. Mol. Cell *48*, 627–640.

Loh, K.M., and Lim, B. (2011). A precarious balance: pluripotency factors as lineage specifiers. Cell Stem Cell *8*, 363–369.

Martin, G.R. (1981). Isolation of a pluripotent cell line from early mouse embryos cultured in medium conditioned by teratocarcinoma stem cells. Proc. Natl. Acad. Sci. USA *78*, 7634–7638.

Mitsui, K., Tokuzawa, Y., Itoh, H., Segawa, K., Murakami, M., Takahashi, K., Maruyama, M., Maeda, M., and Yamanaka, S. (2003). The homeoprotein Nanog is required for maintenance of pluripotency in mouse epiblast and ES cells. Cell *113*, 631–642.

Nichols, J., Zevnik, B., Anastassiadis, K., Niwa, H., Klewe-Nebenius, D., Chambers, I., Scholer, H., and Smith, A. (1998). Formation of pluripotent stem cells in the mammalian embryo depends on the POU transcription factor Oct4. Cell *95*, 379–391.

Nishi, M., Akutsu, H., Masui, S., Kondo, A., Nagashima, Y., Kimura, H., Perrem, K., Shigeri, Y., Toyoda, M., Okayama, A., et al. (2011). A distinct role for Pin1 in the induction and maintenance of pluripotency. J. Biol. Chem. *286*, 11593–11603.

Niwa, H. (2007). How is pluripotency determined and maintained? Development *134*, 635–646.

Niwa, H., Miyazaki, J., and Smith, A.G. (2000). Quantitative expression of Oct-3/4 defines differentiation, dedifferentiation or self-renewal of ES cells. Nat. Genet. *24*, 372–376.

Niwa, H., Masui, S., Chambers, I., Smith, A.G., and Miyazaki, J. (2002). Phenotypic complementation establishes requirements for specific POU domain and generic transactivation function of Oct-3/4 in embryonic stem cells. Mol. Cell. Biol. *22*, 1526–1536.

Rossant, J., and Tam, P.P. (2009). Blastocyst lineage formation, early embryonic asymmetries and axis patterning in the mouse. Development *136*, 701–713.

Ryan, A.K., and Rosenfeld, M.G. (1997). POU domain family values: flexibility, partnerships, and developmental codes. Genes Dev. *11*, 1207–1225.

Saxe, J.P., Tomilin, A., Scholer, H.R., Plath, K., and Huang, J. (2009). Post-translational regulation of Oct4 transcriptional activity. PLoS One *4*, e4467.

Scholer, H.R. (1991). Octamania: the POU factors in murine development. Trends Genet. *7*, 323–329.

Scholer, H.R., Ruppert, S., Suzuki, N., Chowdhury, K., and Gruss, P. (1990). New type of POU domain in germ line-specific protein Oct-4. Nature *344*, 435–439.

Seet, B.T., Dikic, I., Zhou, M.M., and Pawson, T. (2006). Reading protein modifications with interaction domains. Nat. Rev. Mol. Cell Biol. *7*, 473–483.

Shu, J., Wu, C., Wu, Y., Li, Z., Shao, S., Zhao, W., Tang, X., Yang, H., Shen, L., Zuo, X., et al. (2013). Induction of pluripotency in mouse somatic cells with lineage specifiers. Cell *153*, 963–975.

Silva, J., and Smith, A. (2008). Capturing pluripotency. Cell *132*, 532–536.

Smith, A.G. (2001). Embryo-derived stem cells: of mice and men. Annu. Rev. Cell Dev. Biol. *17*, 435–462.

Soldner, F., Stelzer, Y., Shivalila, C.S., Abraham, B.J., Latourelle, J.C., Barrasa, M.I., Goldmann, J., Myers, R.H., Young, R.A., and Jaenisch, R. (2016). Parkinson-associated risk variant in distal enhancer of alpha-synuclein modulates target gene expression. Nature *533*, 95–99.

Spelat, R., Ferro, F., and Curcio, F. (2012). Serine 111 phosphorylation regulates OCT4A protein subcellular distribution and degradation. J. Biol. Chem. *287*, 38279–38288.

Sturm, R.A., Das, G., and Herr, W. (1988). The ubiquitous octamer-binding protein Oct-1 contains a POU domain with a homeo box subdomain. Genes Dev. *2*, 1582–1599.

Swaney, D.L., Wenger, C.D., Thomson, J.A., and Coon, J.J. (2009). Human embryonic stem cell phosphoproteome revealed by electron transfer dissociation tandem mass spectrometry. Proc. Natl. Acad. Sci. USA *106*, 995–1000.

Thomson, J.A., Itskovitz-Eldor, J., Shapiro, S.S., Waknitz, M.A., Swiergiel, J.J., Marshall, V.S., and Jones, J.M. (1998). Embryonic stem cell lines derived from human blastocysts. Science *282*, 1145–1147.

Vigano, M.A., and Staudt, L.M. (1996). Transcriptional activation by Oct-3: evidence for a specific role of the POU-specific domain in mediating functional interaction with Oct-1. Nucleic Acids Res. *24*, 2112–2118.

Wang, C., Chen, Y., Deng, H., Gao, S., and Li, L. (2015). Rbm46 regulates trophectoderm differentiation by stabilizing Cdx2 mRNA in early mouse embryos. Stem Cells Dev. *24*, 904–915.

Young, R.A. (2011). Control of the embryonic stem cell state. Cell *144*, 940–954.

Zhao, Q.W., Zhou, Y.W., Li, W.X., Kang, B., Zhang, X.Q., Yang, Y., Cheng, J., Yin, S.Y., Tong, Y., He, J.Q., et al. (2015). Aktmediated phosphorylation of Oct4 is associated with the proliferation of stemlike cancer cells. Oncol. Rep. *33*, 1621–1629.